Supporting Information

Allenylphosphonium Complexes of Rhodium and Iridium

Ian A. Cade, Annie L. Colebatch, Anthony F. Hill* and Anthony C. Willis

Research School of Chemistry, Institute of Advanced Studies, The Australian National University, Canberra, ACT 0200, Australia

a.hill@anu.edu.au

^{1}H NMR analysis of MCH_2 resonances in allenylphosphonium complexes

The CH_2 region of the ^{1}H NMR spectrum of **[4]PF$_6$** is shown in Figure S1 below. The resonance on the right is assigned to the CH_2 group of the allenylphosphonium ligand of **[4]PF$_6$**. The resonance on the left is the equivalent resonance from the secondary product **[4a]PF$_6$**, the isomer with the CH_2 group *trans* to Cl instead of CO. The resonance is a triplet of doublet of doublets due to coupling to the PPh_3 ligands, the phosphonium group and the methine proton.

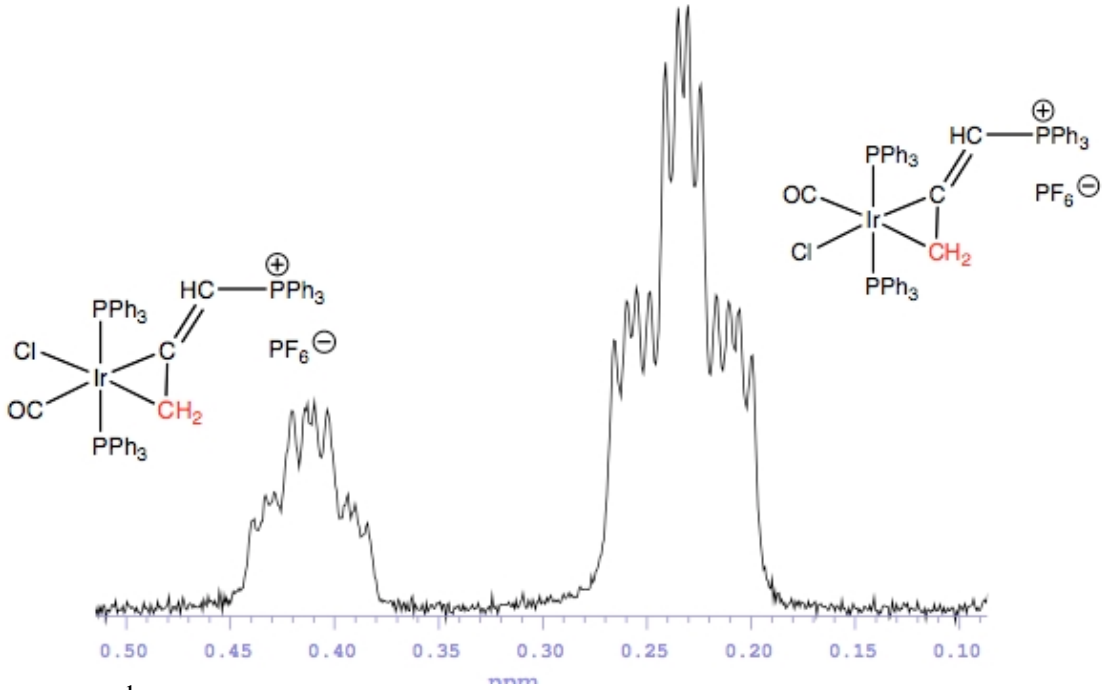

Figure S1. ^{1}H NMR spectrum (0.2 – 0.5 ppm) of crude [4]PF$_6$.

The coupling constants were determined through a series of $^{1}H\{^{31}P\}$ NMR experiments. In the broadband ^{31}P decoupled spectrum, the CH_2 resonance at 0.23 ppm collapsed to a doublet with $^{4}J_{HH}$ = 2.3 Hz, revealing the proton-proton coupling constant. Selective decoupling of the PPh_3 ligands gave a doublet of doublets, from which it was determined that $^{4}J_{PH}$ = 4.5 Hz. Finally, selective decoupling of the phosphonium resonance revealed a triplet of doublets and the coupling constant $^{3}J_{PH}$ = 9.5 Hz. This was verified by a simulated spectrum which closely matches the observed spectrum (**Figure S2**). The coupling constants of **[4a]PF$_6$** were elucidated in the same way. Once these coupling patterns were known, the analogous coupling constants for **[5]PF$_6$** were calculated from the ^{1}H spectrum without the need for additional experiments.

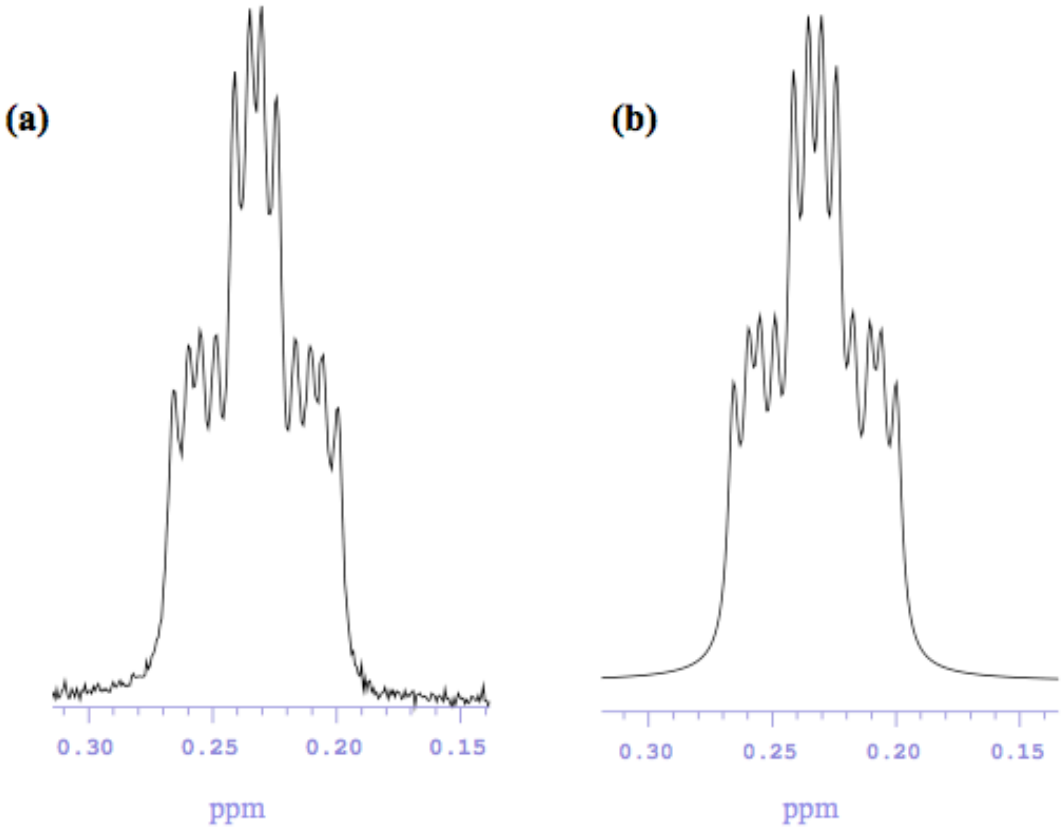

Figure S2. (a) Experimental and (b) simulated ^{1}H NMR spectrum (0.15 – 0.30 ppm) of [4]PF6.

For comparitive purposes, the H NMR spectra showing the equivalent resonances of $[Ru(h^2\text{-}H_2C{=}C{=}CHPPh_3)(CO)_2(PPh_3)_2]_2Br(PF_6)$ and $[Pt(h^2\text{-}CH_2CCHPPh_3)(PPh_3)_2]PF_6$ are included for comparison below.

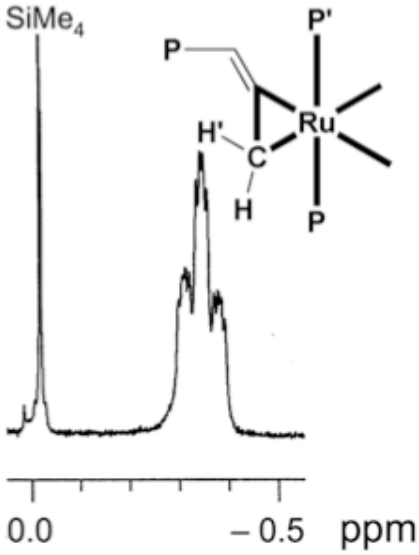

Figure S3. ^{1}H NMR spectrum (0.0 - –0.5 ppm) of $[Ru(\eta^2\text{-}H_2C{=}C{=}CHPPh_3)\text{-}(CO)_2(PPh_3)_2]^+$

The ^{1}H NMR spectrum in Figure S3 shows the CH_2 resonance of $[Ru(\eta^2\text{-}H_2C{=}C{=}CHPPh_3)(CO)_2(PPh_3)_2]^+$. The same distinctive shape as those seen in Figure S1 is evident but the couplings are not as well resolved. Figure S4 shows the CH resonances in the ^{1}H NMR spectra of $[Pt(\eta^2\text{-}CH_2CCHPPh_3)(PPh_3)_2]PF_6$ and $[RhCl(\eta^2\text{-}CH_2CCHPPh_3)(PPh_3)_2]PF_6$. These resonances do not show the same distinctive shape as the iridium and ruthenium examples as a result of the differing nature of the CH_2 environment.

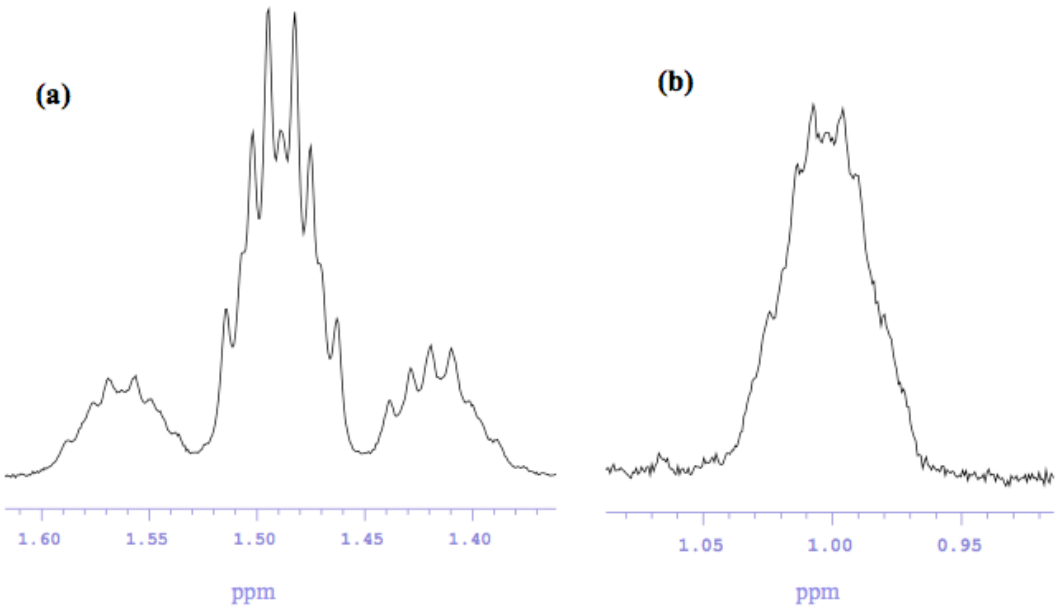

Figure S4. (a) ^{1}H NMR spectrum (1.37 – 1.61 ppm) of $[Pt(\eta^2\text{-}CH_2CCHPPh_3)(PPh_3)_2]PF_6$; (b) ^{1}H NMR spectrum (0.92 – 1.08 ppm) of $[RhCl(\eta^2\text{-}CH_2CCHPPh_3)(PPh_3)_2]PF_6$.